Homogeneous Biogenic Paramagnetic Nanoparticle Synthesis Based on a Microfluidic Droplet Generator**

Jae Hwan Jung, Tae Jung Park, Sang Yup Lee,* and Tae Seok Seo*

The homeostasis process endows microbes with an intrinsic ability to assemble metal ions to form a metal nanoparticle inside. This nanoparticle synthesis strategy inspired from nature can be adapted by using microorganisms as a nanoparticle factory under mild conditions, such as neutral pH, an aqueous phase, and room temperature. Such an eco-friendly biogenic nanoparticle synthesis has advantages over the conventional chemical methods, which require high temperatures, toxic reagents, and large energy sources.[1] In this sense, *Fusarium oxysporum*, *Escherichia coli*, *Actinobacter* sp., and *Staphylococcus aureus* were employed for synthesizing Fe_3O_4, CdS, Fe_3S_4, and Ag nanoparticles in the bulk state.[2–5] However, a limitation of the biogenic nanoparticles is the lack of control over the particle size. Heterogeneous nanoparticles are mainly produced, which may be derived from the different reaction conditions, such as the concentration of the metal ions surrounding each cell.[6,7] As the homogeneity of the nanoparticles, for example paramagnetic nanoparticles, has been demonstrated to be an important factor to be applied for data storage media,[8] ferrofluids,[9] and enhancement agents for magnetic resonance imaging (MRI),[10] the production of the homogeneous biogenic nanoparticles should be accordingly resolved. To overcome polydispersity of biogenic nanoparticles, we used a microfluidics-based droplet generator. The droplet microfluidic systems have been proven as powerful analytical tools by compartmentalizing a number of droplets of femtoliter to microliter volume, by providing uniform and well-defined droplet conditions, and by enabling fast chemical and biological reaction in a high-throughput manner.[11–14] Chemical synthesis of magnetic iron oxide nanoparticle in the droplets was reported to ameliorate the monodispersity owing to the droplet characteristics.[15]

Taking full advantage of droplets, we performed biogenic FeMn magnetic nanoparticle synthesis with the expectation of an improvement of the size homogeneity by precisely tuning the microenvironmental droplet conditions, including cell numbers, concentration of metal ions, and temperature. We prepared the recombinant *E. coli* expressing *Arabidopsis thaliana* phytochelatin synthase (AtPCS) and *Pseudomonas putida* metallothionein (PpMT). Phytochelatin (PC) and metallothionein (MT) are well known as cysteine-rich and heavy-metal-binding proteins. As PCs, which are enzymatically synthesized peptides, and MTs, which are gene-encoded polypeptides, have demonstrated high metal binding affinity and accumulation capacity inside the cells, we genetically designed and engineered *E. coli* to express a PC synthase of *Arabidopsis thaliana* along with an MT of *Pseudomonas putida* for the synergetic effect of the PpMT-AtPCS fusion protein on assembling metal components for nanoparticle synthesis.[16]

A droplet microdevice was designed as shown in Figure 1. There are two aqueous-phase inlets for recombinant *E. coli* cell solution and metal ion solution, and one oil-phase inlet is for introducing FC 40 and surfactant polyethylene glycol perfluoropolyether (PEG-PFPE).[17] For synthesis of FeMn magnetic nanoparticles, we employed $FeSO_4·7H_2O$ and $MnCl_2·4H_2O$ mixture as metal sources, and the flow-focusing structure generated droplets which encapsulate *E. coli* cells and metal ions. They were efficiently mixed when passing through the serpentine microchannel and stored in the droplet incubation chamber for 5 min.
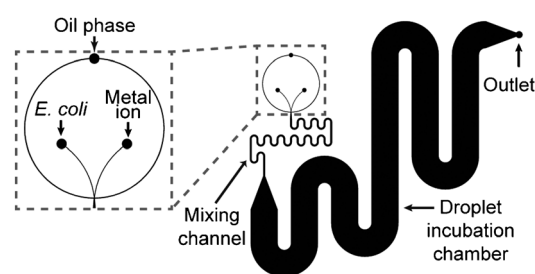

Figure 1. Design of the droplet microdevice for synthesizing biogenic magnetic FeMn nanoparticles.

[*] J. H. Jung,[+] Dr. T. J. Park,[+] Prof. S. Y. Lee, Prof. T. S. Seo
Department of Chemical and Biomolecular Engineering (BK21 program), BioProcess Engineering Research Center, Center for Systems and Synthetic Biotechnology, Institute for the BioCentury, Korea Advanced Institute of Science and Technology (KAIST)
291 Daehak-ro, Yuseong-gu, Daejeon, 305-701 (Republic of Korea)
E-mail: leesy@kaist.ac.kr
seots@kaist.ac.kr
Homepage: http://nanobiomems.kaist.ac.kr

[+] These authors contributed equally to this work.

Supporting information for this article is available on the WWW under http://dx.doi.org/10.1002/anie.201108977.

As shown in Figure 2a, homogeneous droplets with 250 μm diameter and 65.4 nL volume were generated and incubated. The encapsulated *E. coli* cells stained with LIVE/DEAD BacLicght bacterial viability kit (Molecular Probes, NY, USA) were visualized as a green color in the droplets under the laser-induced confocal microscope (C1si, Nikon,

5634
WILEY ONLINE LIBRARY

© 2012 Wiley-VCH Verlag GmbH & Co. KGaA, Weinheim

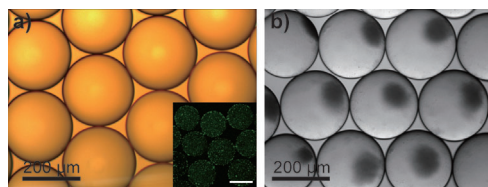*Angew. Chem. Int. Ed.* **2012**, *51*, 5634–5637

Figure 2. a) Optical image of the homogeneous droplets (diameter 250 μm) containing the recombinant *E. coli*, and the fluorescent image of the stained cells in the droplet (inset; scale bar: 200 μm); b) optical image of the droplets in which the recombinant *E. coli* synthesized FeMn magnetic nanoparticles after 18 h incubation.

Figure 4. a) Representative FE-TEM image of the recombinant *E. coli* containing biogenic FeMn nanoparticles recovered from the droplets; b) elemental analysis of FeMn nanoparticles by EDXS.

Japan). The cell number was estimated as 3.32×10^5 per droplet, and most of cells were observed as well-dispersed green dots, which mean they were alive (inset of Figure 2 a). After 5 min in the droplet incubation chamber, the droplets were stably collected at the outlet without breakage. The recovered droplets were further incubated at 37 °C for 18 h. As shown in Figure 2 b, the droplets containing the cells and metal ions maintained their shape (diameter 250 μm), and the color of the cell was changed from bright yellow to brown as the biogenic nanoparticles were synthesized inside the cells.

To confirm the biogenic nanoparticle synthesis inside the *E. coli* cells, we controlled the movement of *E. coli* cells in the droplets by applying a magnet field. The cells, which were initially uniformly dispersed in the droplets, were attracted and concentrated toward either the left side (Figure 3 a) or right side (Figure 3 b) by an external magnet. After breakage of droplets by using a droplet destabilizer, the *E. coli* containing FeMn nanoparticles were collected in an Eppendorf tube. When the magnet was placed against the tube wall, the cells attached to the wall and were dragged to the magnet. After displacement of a magnet, the trace of the cells on the wall could be clearly seen (Supporting Information, Figure S1). Therefore, these results demonstrated that the recombinant *E. coli* was able to synthesize a biogenic FeMn magnetic nanoparticle inside the droplets successfully.
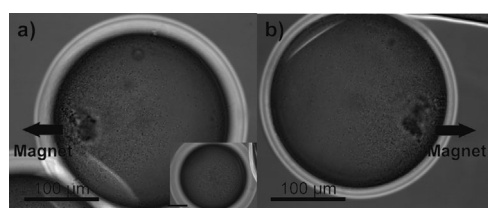

Figure 3. Optical images of cell movement in the incubated droplets. The recombinant *E. coli* was moved to a) the left side and b) the right side according to the direction of an external magnet, demonstrating that the biogenic FeMn magnetic nanoparticles were synthesized in the cells. The inset of (a) shows the randomly dispersed *E. coli* in the absence of the magnetic field.

The obtained recombinant *E. coli* cells were washed in PBS by ultracentrifugation and analyzed by field emission transmission electron microscope (FE-TEM). Although the exact shape of the FeMn nanoparticles was not clearly shown in the *E. coli* (Figure 4 a) owing to the metal binding proteins
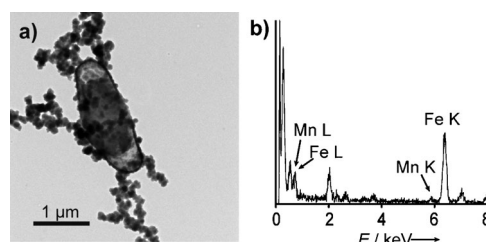
and salt aggregation, the synthesized FeMn nanoparticles could be identified as a gray color. The nanoparticles mainly existed inside the cells, while the black dots which indicated salt aggregation were present outside the cells. We performed the compositional analysis of the nanoparticles by using energy-dispersive X-ray spectroscopy (EDXS). As shown in Figure 4 b, the existence of Fe (0.71 and 6.40 keV) and Mn (0.64 and 5.89 keV) peaks was detected. Despite the same feeding concentration of $FeSO_4 \cdot 7 H_2O$ and $MnCl_2 \cdot 4 H_2O$ (5 mM) used, the relative peak intensity of Fe at 6.40 keV was significantly higher than that of Mn at 5.89 keV, indicating the preference of phytochelatin and metallothionein metal binding proteins to uptake Fe rather than Mn for nanoassembly. The element peak of Mn L (0.64 keV) overlapped with Fe L peak (0. 71 keV) were shown together with C (0.27 keV), O (0.52 keV), N (0.39 keV), and S (2.31 keV) element peaks that were derived from the metal binding protein of the *E. coli* cells.

To investigate the homogeneity of the produced biogenic FeMn nanoparticles, we performed calcination at 680 °C for 2 h for thermal decomposition of the heavy proteins bound to the surface of nanoparticles. The isolated biogenic nanoparticles were analyzed by FE-TEM as shown in Figure 5. As a reference, we generated the biogenic FeMn nanoparticles on the off-chip base under the same experimental conditions as above (Supporting Information, Figure S2). The *E. coli* cells incubated in the bulk state were moved by an external magnet and the cells displayed the FeMn nanoparticles. The EDXS analysis data on the FeMn nanoparticles was similar to that of Figure 4 b. Regarding size distribution, the off-chip-based FeMn nanoparticles represented polydispersity with a diameter of (3.04 ± 0.68) nm, while the droplet-based biogenic nanoparticles showed an threefold improved homogeneity of (5.17 ± 0.24) nm (Figure 5 a). The size of biogenic nanoparticle could be tuned by controlling the concentration of the metal ion solution.[16] High-resolution TEM (HRTEM) analysis revealed that the FeMn biogenic nanoparticles had a well-defined crystalline structure with an interplanar distance of 3.30 Å in both the on-chip (Figure 5 b) and off-chip synthetic methods. Statistical analysis of the nanoparticle size revealed that the droplet-based nanoparticles showed a narrow size distribution by plotting over 95 % of the nanoparticles localized in the average size of 5.17 nm (Figure 5 c), while that of the bulk phase synthesis displayed a wider distribution ranging from 1 nm to 4.5 nm. With the assumption that the activity of metal binding protein is
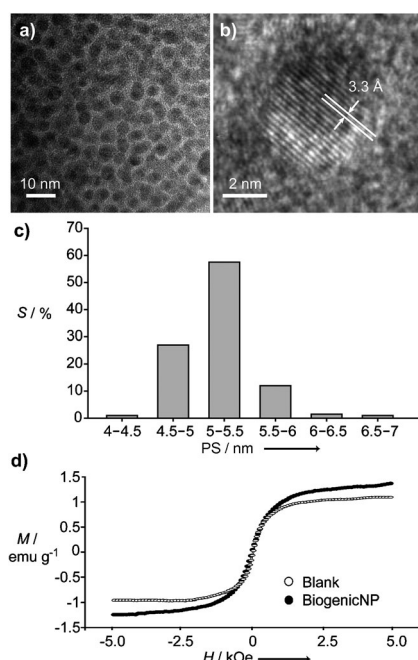
Figure 5. a) Representative TEM image of homogeneous FeMn biogenic nanoparticles (average diameter: 5.17 nm) synthesized by the recombinant *E. coli* in the droplet microfluidic system; b) HRTEM image of an FeMn nanoparticle; c) size distribution *S* of the produced FeMn nanoparticles (PS = particle size); and d) VSM analysis to investigate the magnetization *M* of the biogenic FeMn nanoparticles at magnetic field *H*.

equivalent in the recombinant *E. coli*, the improvement of size homogeneity can be attributed to the droplet microfluidic system. As the droplet provides a nanoliter-scale bioreactor platform with high uniform microenvironments, the encapsulated *E. coli* would experience the same concentration of metal ions and incubation time which lead to the homogeneous nanoparticle synthesis. In contrast, the bulk phase can give rise to the concentration fluctuation surrounding the cells, so that each cell would accept the metal ions differently, thereby generating biogenic nanoparticles with a wide range of size distribution (Supporting Information, Figure S3).

The magnetic properties of the isolated FeMn biogenic nanoparticles was characterized by a vibrating sample magnetometer (VSM) analysis. As shown in Figure 5d, the magnetization profile of the biogenic nanoparticles was distinguished from that of the blank sample. The FeMn nanomagnetity was unsaturated without losing the magnetic properties in the range from −5.0 to 5.0 kOe, proving these FeMn biogenic nanoparticles are paramagnetic.

In conclusion, we have demonstrated the improvement of the size homogeneity of the biogenic magnetic FeMn nanoparticles by using a microfluidic droplet generator. The recombinant *E. coli* expressing metal binding proteins of AtPCS and PpMT served as a nanoparticle factory. The droplet microfluidic technology can produce a number of the homogeneous droplets, the equivalent number of cells, and the same metal ion concentrations in each droplet. This precise controllability for microenvironments enables the recombinant *E. coli* cells to assemble the metal ion under the

quite similar conditions, resulting in the homogeneous biogenic FeMn magnetic nanoparticles. Therefore, the heterogeneous size distribution of the conventional bulk-phase-based biogenic nanoparticle could be overcome by utilizing the advantages of the microfludic system. Moreover, our study truly demonstrated the use of the droplet as a nanoliter bioreactor in which the cells were incubated and worked for nanoassembly. Since the scale-up of the droplets is currently under way,[18–20] it is a promising method to produce homogenous biogenic nanoparticles in an eco-friendly, cost-effective, and highly parallel process.

Experimental Section

Luria–Bertani (LB) medium was obtained from BD Difco (Franklin Lakes, NJ, USA). Ampicillin, isopropyl-β-D-thiogalactopyranoside (IPTG), iron(II) sulphate heptahydrate, manganese(II) chloride tetrahydrate, and phosphate-buffered saline (PBS) were purchased from Sigma–Aldrich (St. Louis, MO, USA). Fluorocarbon oil FC40 was ordered from 3M (Hermeslaan, Belgium). An EA surfactant, which consisted of polyethylene glycol and perfluoropolyether, and a droplet destabilizer were from RainDance technology (Lexington, MA, USA).

Construction of recombinant *E. coli* DH5α strains harboring pTJ1-PpMT:AtPCS: The information of strains and plasmids and PCR primers are listed in the Supporting Information, Table S1 and S2, respectively. The DNA fragment encoding PpMT was amplified using the genomic DNA of *P. putida* KT2440 as a template and the primers P1 and P2, and then digested with *Eco*RI and *Pst*I, and ligated into pTac99A plasmid to make pTJ1-PpMT-T.[21] The DNA fragment encoding AtPCS was amplified by the polymerase chain reaction using the cDNA library of *A. thaliana* ecotype Columbia (leaves) as a template and the primers P3 and P4, and digested with *Pst*I and *Hin*dIII, and ligated into pTJ1-PpMT-T, yielding pTJ1-PpMT:AtPCS. The DNA sequences of all clones were confirmed by the automatic DNA sequencer (PerkinElmer).

Cell cultivation: A 100 μL of the recombinant *E. coli* was incubated in 10 mL of LB medium containing ampicillin (50 μg mL^{-1}) for 18 h at 37°C with 200 rpm stirring rate. After incubation, 1 mL of the incubated *E. coli* solution was incubated again with a 100 mL of LB medium for 2 h 30 min for proliferation of the cells. Then, the concentration of the cell solution was measured by a UV/Vis spectrophotometer (UV-2450, SHIMADZU, Japan). When the absorbance value at 600 nm, OD$_{600}$, was reached at 0.4, 1 mM IPTG was added for induction of phytochelatin synthase and metallothionein metal-binding protein. After further incubation for 90 min, the cells were washed three times with PBS (pH 7.4) and concentrated to a 10 mL solution with a final concentration of 5.072×10^9 cells mL^{-1}.

Chip fabrication: The microfluidic channel was fabricated with poly(dimethylsiloxane) (PDMS) using a conventional soft-lithography method. As a mold master, SU-8 50 photoresist (MicroChem, MA, USA) was spin-coated on a 10 cm silicon wafer and the channel pattern of a photomask was transferred by UV exposure. After development, microchannels with 100 μm depth were generated. Then, the prepolymer of PDMS and curing agent (Sylgard 184, Dow corning, MI, USA) were mixed with a 10:1 ratio and poured onto the master. After curing at 65°C for 2 h, the PDMS layer was peeled off from the mold. Finally, the patterned PDMS layer was treated with oxygen plasma for 1 min and permanently bonded with a monolithic PDMS membrane.

Cell encapsulation and incubation: Droplets were generated by a flow-focusing structure and the contents in the droplets were efficiently mixed in the serpentine microchannel. A metal ion and *E. coli* solution were merged at the center and encapsulated in droplets with background of FC40 oil phase which contains 1.8% w/w EA

surfactant. For biogenic FeMn nanoparticle synthesis, degassed 5.0 mM iron(II) sulphate heptahydrate (FeSO$_4$·7H$_2$O) and manganese(II) chloride tetrahydrate (MnCl$_2$·4H$_2$O) were employed. Prior to injection of aqueous and oil phases, the microfluidic device was coated with hexamethyldisilazane for 15 min to increase the hydrophobicity of the microchannels. The flow rate of the *E. coli* and metal ion solution was 4 µL min^{-1}, while that of FC 40 oil phase was 15 µL min^{-1}, which were stably controlled by using syringe pumps (KD Scientific Inc., Holiston, MA, USA). Under these conditions, the droplets which had 250 µm diameter and 65.4 nL volume were continuously generated, and the encapsulated droplets containing the recombinant *E. coli* cells and metal ion solutions were collected at the outlet without disruption. The droplets were incubated at 37 °C for 18 h to proceed the biogenic nanoparticle synthesis.

Isolation of the biogenic FeMn nanoparticles: Incubated droplets were transferred to a 1.5 mL tube, and then a droplet destabilizer was added and vortexed. After centrifugation at 13 000 rpm for 10 min, the precipitated *E. coli* cells were recovered and washed with a PBS (pH 7.4) buffer three times. Harvested cells were calcinated at 680 °C for 2 h to thermally decompose the proteins bound on the nanoparticles.

Characterization of biogenic FeMn nanoparticles: The purified FeMn nanoparticles were characterized by field emission transmission electron microscope (FE-TEM, Tecnai G^2 F30 S-Twin, FEI) operated at an accelerating voltage of 300 kV. Magnetic measurements were carried out using a vibrating sample magnetometer (VSM, 2900-02 AFIM, PMC Co.).

[1] T. Hyeon, *Chem. Commun.* **2003**, 927–934.
[2] A. Bharde, D. Rautaray, V. Bansal, A. Ahmad, I. Sarkar, S. M. Yusuf, M. Sanyal, M. Sastry, *Small* **2006**, *2*, 135–141.
[3] S. H. Kang, K. N. Bozhilov, N. V. Myung, A. Mulchandani, W. Chen, *Angew. Chem.* **2008**, *120*, 5264–5267; *Angew. Chem. Int. Ed.* **2008**, *47*, 5186–5189.
[4] A. A. Bharde, R. Y. Parikh, M. Baidakova, S. Jouen, B. Hannoyer, T. Enoki, B. L. V. Prasad, Y. S. Shouche, S. Ogale, M. Sastry, *Langmuir* **2008**, *24*, 5787–5794.
[5] A. Nanda, M. Saravanan, *Nanomedicine* **2009**, *5*, 452–456.
[6] J. R. S. Newman, S. Ghaemmaghami, J. Ihmels, D. K. Breslow, M. Noble, J. L. DeRisi, J. S. Weissman, *Nature* **2006**, *441*, 840–846.
[7] N. Q. Balaban, J. Merrin, R. Chait, L. Kowalik, S. Leibler, *Science* **2004**, *305*, 1622–1625.
[8] G. Reiss, A. Hutten, *Nat. Mater.* **2005**, *4*, 725–726.
[9] K. Raj, B. Moskowitz, R. Casciari, *J. Magn. Magn. Mater.* **1995**, *149*, 174–180.
[10] S. Mornet, S. Vasseur, F. Grasset, E. Duguet, *J. Mater. Chem.* **2004**, *14*, 2161–2175.
[11] L.-H. Hung, K. M. Choi, W.-Y. Tseng, Y.-C. Tan, K. J. Shea, A. P. Lee, *Lab Chip* **2006**, *6*, 174–178.
[12] H. Song, D. L. Chen, R. F. Ismagilov, *Angew. Chem.* **2006**, *118*, 7494–7516; *Angew. Chem. Int. Ed.* **2006**, *45*, 7336–7356.
[13] B. T. Kelly, J.-C. Baret, V. Taly, A. D. Griffiths, *Chem. Commun.* **2007**, 1773–1788.
[14] S.-Y. Teh, R. Lin, L.-H. Hung, A. P. Lee, *Lab Chip* **2008**, *8*, 198–220.
[15] L. Frenz, A. E. Harrak, M. Pauly, S. Begin-Colin, A. D. Griffiths, J.-C. Baret, *Angew. Chem.* **2008**, *120*, 6923–6926; *Angew. Chem. Int. Ed.* **2008**, *47*, 6817–6820.
[16] T. J. Park, S. Y. Lee, N. S. Heo, T. S. Seo, *Angew. Chem.* **2010**, *122*, 7173–7178; *Angew. Chem. Int. Ed.* **2010**, *49*, 7019–7024.
[17] C. Holtze et al., *Lab Chip* **2008**, *8*, 1632–1639 (see the Supporting Information).
[18] X. Casadevall i Solvas, A. deMello, *Chem. Commun.* **2011**, *47*, 1936–1942.
[19] http://www.raindancetech.com/products/ RainDanceRDT1000SellSheet.pdf.
[20] Y. Zeng, R. Novak, J. Shuga, M. T. Smith, R. A. Mathies, *Anal. Chem.* **2010**, *82*, 3183–3190.
[21] S. J. Park, S. Y. Lee, *J. Bacteriol.* **2003**, *185*, 5391–5397.